Research Article

Journal of Environmental Nanotechnology

Generating a Multiple Focal Hole using a Phase-modulated Azimuthally Polarized Laguerre-Bessel-Gaussian Beam

J. William Charles[1], M. Udhayakumar[1], K. B. Rajesh[1*], M. Lavanya[2], A. Mohamed Musthafa[3]

[1]Department of Physics, Chikkanna Government Arts College, Tiruppur, TN, India
[2]Department of Physics, PSGR Krishnammal College for Women, Coimbatore, TN, India
[3]Department of General Studies, Jubail University College, Royal Commission of Jubail, Saudi Arabia

Received: 21.08.2019 Accepted: 25.09.2019 Published: 30-09-2019

*rajeshkb@gmail.com

ABSTRACT

A technique has been suggested for creating many sub-wavelength focal hole segments by tightly focusing a phase-modulated Azimuthally Polarized Laguerre-Bessel-Gaussian Beam (APLBGB). Vector diffraction theory was used to explore the focusing properties. It has been found that by properly controlling the phase of the incident azimuthally polarized light, a focal hole segment with several focal structures separated by varying axial distances can be constructed. Such focused patterns are expected to be beneficial in atom optics, optical manipulations and multiple optical traps.

Keywords: Fluoerscence microscopy.

1. INTRODUCTION

The three-dimensional gradient force optical tweezers demonstrated by Ashkin *et al.* in 1986 have proven to be useful tools for manipulating microscopic objects with a refractive index higher than that of the surrounding medium (high index particle) (Sasaki *et al.* 1992). Such tweezers, however, cannot be used for trapping microscopic particles of refractive index lower than that of the surrounding medium (low index particles) because these get repelled away from the regions of the highest intensity. The ability to trap and manipulate such low-index Particles would allow for the trapping of bubbles and droplets to investigate their evolution in different liquid media since low index particles such as bubbles are of considerable interest for their potential application in the field of biology, medicine and environmental science. For example, recently, enhancement of cell permeability caused by localized cell damage induced by the asymmetric collapse of a bubble has been used for drug delivery and transfection of genes into the living cells (Gahagan and Swartzlander, 1996). Since the cavitation damage by a collapsing bubble depends on its relative to trap and manipulate low index particles (Ashkinn and Dziedzic, 1989) may enhance the understanding of bubble dynamics and optimize the extent of the cell damage caused by bubbles. Similarly, low index particles are also finding use as contrast agents (Wright *et al.* 1990) and for selective destruction of cancer cells (Tadir *et al.* 1990) separation from the surface. Moreover, the conventional gradient-force trap based on the design of Ashkin *et al.* has some limitations, such as the trapped particles are susceptible to optical damage by absorptive heating because the centre of the trap is located in the high-intensity focal region of the beam. This hinders the earlier suggestion of biomedical and related applications involving micromanipulation of living cells (Block *et al.* 1990) chromosomes (Swoboda *et al.* 1993), spermatozoa (Tacgubana *et al.* 1999) and motor proteins. (Ye *et al.* 2004; Prentice *et al.* 2005). One basic approach for trapping low index particles is to generate a region of lower intensity, surrounded by a higher intensity region. Optical bottle fields also have applications in stimulated emission depletion (STED) fluorescence microscopy (De Jong *et al.* 2002), in which the three-dimensional nature of the bottle provides enhanced resolution along the longitudinal direction (Hell and Wichmann, 1994; Lenz *et al.* 1994). Various techniques have been proposed to generate bottle fields (Suyama and Zhang, 2013; Shvedov *et al.* 2008; Chen *et al.* 2004; Zhang *et al.* 2011). Many of these involve vortices generated by phase masks, spiral phase plates, or spatial light modulators (Loiko *et al.* 2013; Gbur and Visser, 2003). These methods typically rely on interference between two fundamental Gaussian modes, making them sensitive to alignment errors (Mahou *et al.* 2015). Tovar presented novel Laguerre–Bessel–Gaussian (LBG) beam as a solution to the paraxial wave equation in cylindrical dimensions in the year 2000. (Tovar, 2000). The LBG beams can reduce to the BG modes and LG modes by properly tuning the initial parameters. Subsequently, the non-paraxial propagation properties of vectorial LBG beams were researched based on vectorial Rayleigh–Somerfield formulae (Mei and Zhao, 2007). Recently, the Vector Diffraction theory was used to investigate the tight focusing properties of radially polarised

Laguerre–Bessel–Gaussian beams by a high numerical aperture objective in an immersion liquid. Based on Vector Diffraction theory, the authors have proposed a unique method for trapping low refractive index particles with an azimuthally polarised Laguerre-Bessel-Gaussian Beam, phase-modulated with well-optimized phase filters in this study. It has been discovered that by appropriately modifying the phase of the incident beam with a multi-belt complex phase filter (MBCPF), multiple focal hole patterns with different sub-wavelength dimensions and large focal depths can be generated, which find applications in a variety of optical trapping and atom optics applications.

2. THEORY

The investigation was carried out by numerically analysing Richards and Wolf's Vectorial Diffraction equation, which is extensively being utilised in high NA focusing systems (Richards and Wolf, 1959). The incident azimuthally polarised beam's electric field distribution in the area of focus is given by,

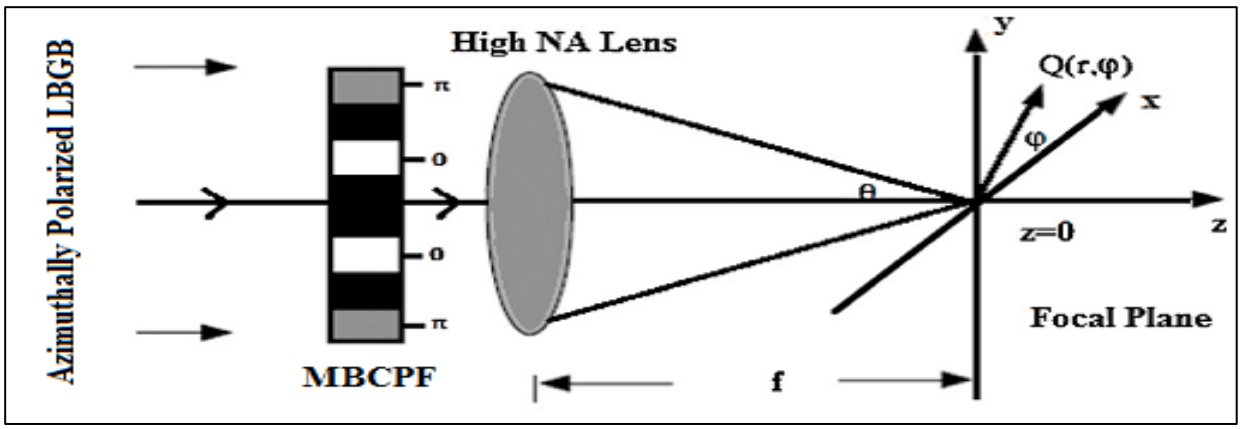

Fig. 1: Tight focusing properties of azimuthally polarized Laguerre-Bessel-Gaussian beam passing through a complex phase filter and focused by a high-NA lens

$$E(r,\varphi,z)=\begin{bmatrix}E_r\\E_\varphi\\E_z\end{bmatrix}=\left[2A\int_0^{\alpha}\cos^{1/2}(\theta)\sin(\theta)\,\mathrm{A}(\theta)\,\mathrm{J}_1(kr\sin\theta)\,\mathrm{e}^{ikz\cos\theta}\right]d\theta\rightarrow(1)$$

where, A is relative amplitude, θ_{max} = *arcsin (NA/n*) that is the maximum aperture angle with (NA/n) is the ratio of numerical aperture (NA), and n is the index of refraction between the lens and the sample. *k* is the wavenumber in free space. $J_n(\theta)$ denotes the nth order Bessel function and the function of T*(θ)* describes the amplitude modulation. In the focusing system with a high NA objective lens, the focusing beam of light is an azimuthally polarized LBG beam. In the cylindrical coordinate system (r, φ, z), the pupil function *l(θ)* for an azimuthally polarized LBG beam at the source plane z = 0, can be defined as (Mei and Zhao, 2007),

$$l(\theta)=\frac{\beta^2\sin\theta}{\sin\theta_{\max}}L_0^1\left(\frac{2\beta^2\sin^2\theta}{\sin\theta_{\max}}\right)J_1\left(2\beta\frac{\sin\theta}{\sin\theta_{\max}}\right)\times\exp\left(-\frac{\beta^2\sin^2\theta}{\sin\theta_{\max}}\right)\rightarrow(2)$$

with β, which is the truncation parameter defined as the ratio of pupil to beam waist in front of the focusing objective. *θmax = arcsin(NA/n)* represents the maximum value of the convergence angle θ, n is the refraction in the image plane, L_0^1 denotes the Laguerre polynomial with the radial and angular modes of 0 and 1, and J_1 is the Bessel function of the first kind of order one, respectively.

Fig. 1 depicts the dedicated Multi-complex Phase Filter (MBCPF). The MBCPF is a phase and amplitude filter with four belts in the radial direction. They are believed to be the most effective DOEs for reducing focal spot size and increasing focal depth (Prabakaran *et al.* 2014). The effect of multi-belt complex phase filter on the input azimuthally polarized LBGB can be evaluated by,

$$T(\theta) = \begin{cases} 0, \ for 0 < \theta < \theta_1, \theta_2 < \theta < \theta_3, \\ 1, \ for \theta_1 < \theta < \theta_2, \\ -1 \ for \theta_3 < \theta < \theta_{max} \end{cases} \rightarrow (3)$$

In this situation, the authors looked at the four-belt spiral phase hologram, and the set of four angles was optimized to generate a certain focused pattern using a standard global-search-optimization methodology (Wang *et al.* 2008). Based on this algorithm, one structure with random values for θ_1 to θ_3 was chosen from all the possibilities; then Vector Diffraction theory was used to quantitatively model their focusing characteristics. If the structure produced a sub-wavelength single focus spot as predicted, meeting the limiting constraints that the Full Width Half Maximum (FWHM) of the generated focal spot segment is less than 0.5λ, it was used as the starting structure for the optimization operations. In the following steps, varying θ of one chosen zone was continued slowly and precisely to generate multiple focal spot segments while adhering to the limiting conditions that the FWHM of each generated focal spot is less than 0.5λ and that there are at least five, three or two such focal spots in the focal segment.

3. RESULTS AND DISCUSSION

Fig. 1 depicts a schematic representation of the suggested approach. The numerical evaluation of Eq. (6.1) was carried out by setting λ as 1 and the objective's NA to 0.95. For the sake of simplicity, it was assumed that the focusing was on air, with a refractive index n of 1 and a refractive amplitude A of 1. In the following phase, it was continued to increase the value θ of the chosen zone in order to construct a double focus hole segment while keeping the limiting condition constant. Fig. 2 illustrates the formation of two focal hole segment generated by the high NA lens for the CPF optimized with angle $\theta_1 = 50.90^{\circ}$, $\theta_2 = 56.85^{\circ}$ and $\theta_3 = 60.83^{\circ}$ for β = 1.1. According to Fig. 2 (c), each created focal hole has a focal depth of about 4.4λ and an FWHM of 0.37. The axial distance between two focal hole constructions is 2.1λ and was measured at r = 0.35λ, as illustrated in Fig. 2 (b).

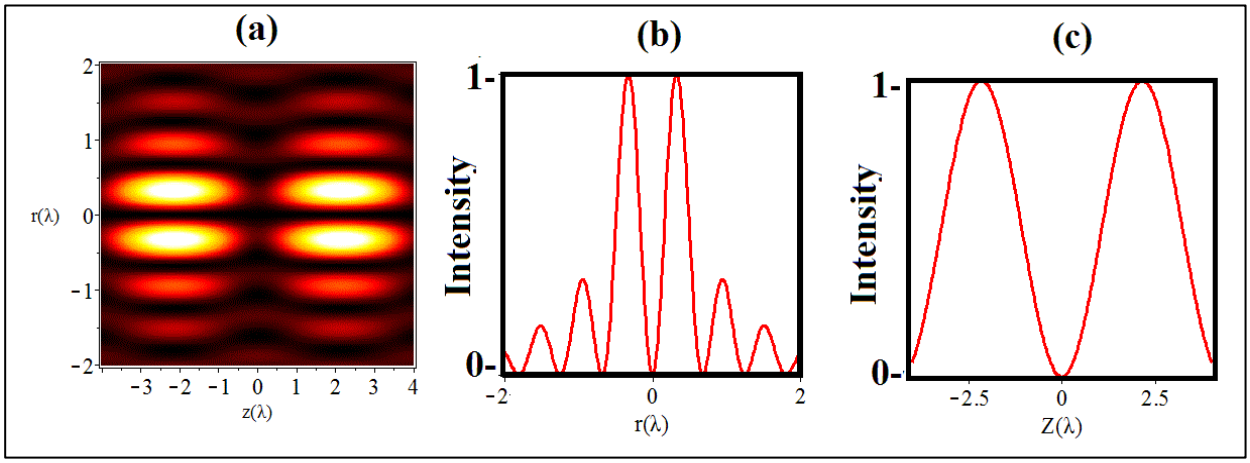

Fig. 2: (a) The 2D normalized intensity distribution in the r- z plane (b) The total intensity distribution at z = 2.1λ and (c) The axial intensity distribution at r = 0.35λ

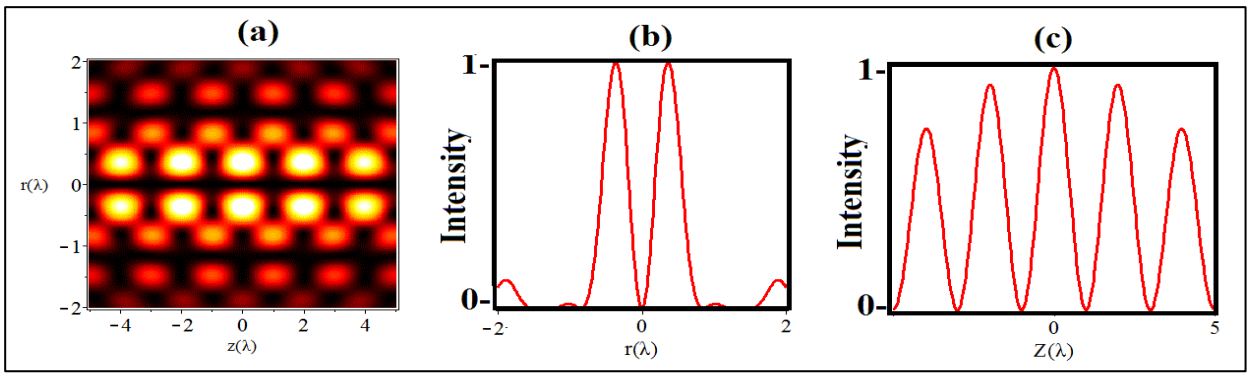

Fig. 3: (a) The normalized intensity distribution in the r- z plane (b) The total intensity distribution at z = 2λ and (c) The axial intensity distribution at r = 0.35λ

Fig. 3 shows the multiple focal hole segment generated by the high NA lens for the CPM with for β = 1.1. It was observed from the figure that the generated focal segment contained an array of five focal hole, each having FWHM of 0.37 λ with d around 1.2 λ and were axially separated by the distance z = 2λ. These angles were optimized based on the procedure mentioned for Fig. 6.2, but with the limiting condition that the FWHM of the generated focal hole segment was less than 0.5 and there should be at least five such focal holes in the focal segment.

Fig. 4 shows the possibility of obtaining series of sub-wavelength scale focal hole segments of slightly different FWHM aligned alternatively along the axial direction. We noted that such a focal segment could be generated with the CPF optimized with angle θ_1= 39.06°, θ_2= 42.12°, and θ_3= 60.83°. Fig. (3b) shows the FWHM of inner focal holes was 0.38λ, where the larger located alternatively to this was FWHM of 0.8λ. The axial intensity measured at r=0.35λ has shown that the intensity of the focal hole at the focus was maximum and faded exponentially along the longitudinal axis.

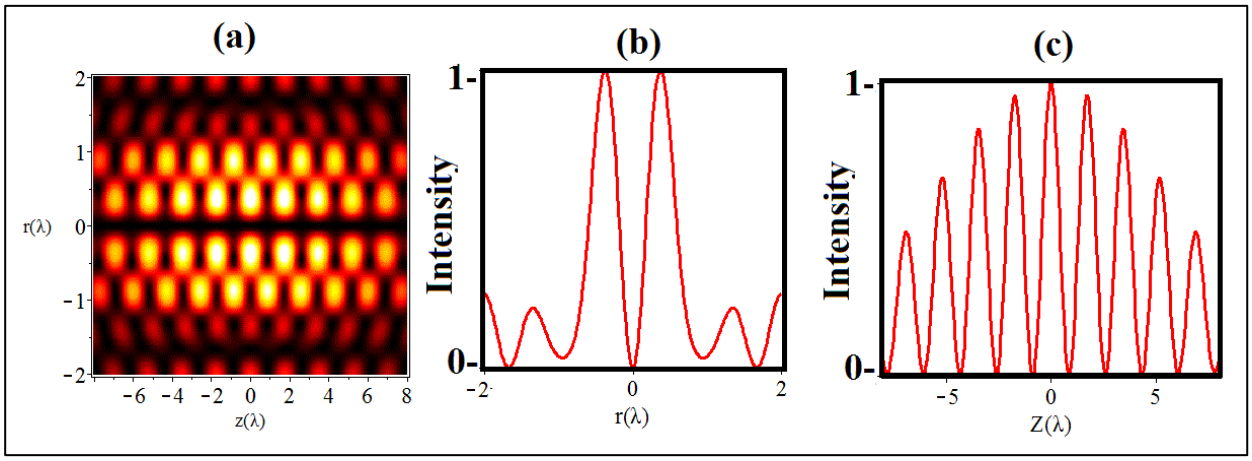

Fig. 4: (a) The normalized intensity distribution for multiple focal hole segment (b) The total intensity distribution at z = 0 and (c) The axial intensity distribution at r = 0.35

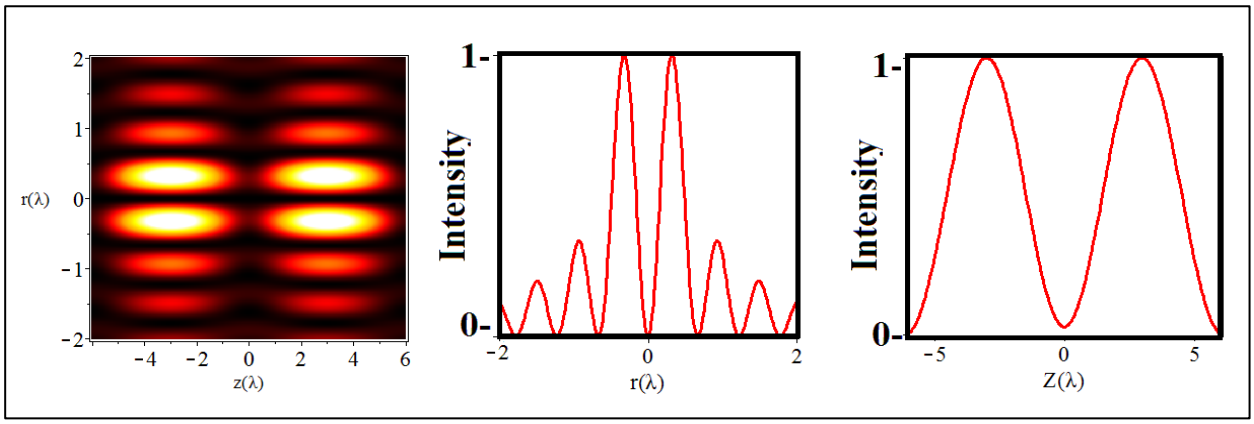

Fig. 5: (a) The normalized intensity distribution in the r- z plane (b) The total intensity distribution at z = 3λ (c) The axial intensity distribution at r = 0.35λ

Fig. 5 (a) shows that the focal segment obtained for the CPF optimized with angle θ_1= 36.06^0, θ_2= 41.12° and θ_3= 48.83°. It was observed from the figure that the generated focal hole was having FWHM of 0.33λ and a focal depth of 2.8λ. It was noted the axial intensity of the focal hole is equal and was axially separated by the distance 2.5λ. As a result, an array of almost equally intense and regularly spaced sub-wavelength focus hole segments that can be utilized to capture two low refractive index particles at the same time may be constructed. Thus, by varying the pupil beam ratio of the incoming LBG for a well-optimized complex phase filter, numerous new focused patterns suited for capturing several low refractive index particles may be generated.

Table 1. Focal patterns obtained for phase-modulated APLBG beam

S. No.	APLBGB (β)	Optimized angle of CPF	Number of focal holes	FWHM (λ)	DOF (λ)	Axial separation (λ)
1	1.1	θ_1=50.90°, θ_2= 56.85° and θ_3= 6°.83°	2	0.37	4.4	2.5
2	1.1	θ_1= 39.06°, θ_2= 42.12° and θ_3= 48.83°	5	0.37	1.2	2
3	1.1	θ_1= 39.06°, θ_2= 42.12° and θ_3= 60.83°	9	0.34	0.8	2
4	1.1	θ_1= 56.06°, θ_2= 58.12° and θ_3= 60.83°	2	0.35	2.8	3.1

.

4. CONCLUSION

The tight focusing capabilities of azimuthally polarised LBGB focused through a well-optimized complex phase filter were numerically shown using Vector Diffraction theory. Numerical results have demonstrated that by varying the phase of the CPF and the pupil beam ratio of the incident APLBGB, several innovative focused patterns may be achieved such as the splitting of a focal hole segment into an array of two or five focal hole segments. It has also been discovered that the focal segment with somewhat varied FWHM may be positioned evenly and alternately.

FUNDING

This research received no specific grant from any funding agency in the public, commercial, or not-for-profit sectors.

CONFLICTS OF INTEREST

The authors declare that there is no conflict of interest.

REFERENCES

Ashkin, A. and Dziedzic, J. M., Optical trapping and manipulation of single living cells using infra-red laser beams, *Ber. Bunsenges. Phys. Chem*., 93(3), 254 (1989). https://dx.doi.org/10.1002/bbpc.19890930308

Block, S. M., Goldstein, L. S. and Schnapp, B. J., Bead movement by single kinesin molecules studied with optical tweezers, *Nature (London)*, 348-352(1990). https://dx.doi.org/10.1038/348348a0

Chen, C.-H., Tai, P.-T. and Hsieh, W.-F., Bottle beam from a bare laser for single-beam trapping, *Appl. Opt.*, 43(32), 6001–6006(2004).

De Jong, N., Bouakaz, A. and Frinking, A., Echocardiography, 19(3), 229 (2002). https://dx.doi.org/10.1046/j.1540-8175.2002.00229.x

Gahagan, K. T. and Swartzlander, G. A., Optical vortex trapping of particles, *Opt. Lett*., 21(11), 827-829(1996). https://dx.doi.org/10.1364/OL.21.000827

Gbur, G. and Visser, T. D., Coherence vortices in partially coherent beams, *Opt. Comm*., 222(1-6), 117–125(2003). https://dx.doi.org/10.1016/S0030-4018(03)01606-7

Hell, S. W. and Wichmann, J., Breaking the diffraction resolution limit by stimulated emission: stimulated-emission depletion fluorescence microscopy, *Opt. Lett*., 19(11), 780–782(1994). https://dx.doi.org/10.1364/OL.19.000780

Lenz, M. O., Sinclair, H. G., Savell, A., Clegg, J. H., Brown, A. C., Davis, D. M., Dunsby, C., Neil, M. A. and French, P. M., 3-D stimulated emission depletion microscopy with programmable aberration correction, *J. Biophotonics*, 7(1-2), 29–36 (2014). https://dx.doi.org/10.1002/jbio.201300041

Loiko, Y. V., Turpin, A., Kalkandjiev, T., Rafailov, E.U. and Mompart, J., Generating a three-dimensional dark focus from a single conically refracted light beam, *Opt. Lett*., 38(22), 4648–4651 (2013). https://dx.doi.org/10.1364/OL.38.004648

Mei, Z. and Zhao, D., Nonparaxial analysis of vectorial Laguerre–Bessel–Gaussian beams, *Opt. Express*, 15(19), 11942–11951(2007). https://dx.doi.org/10.1364/OE.15.011942

Prabakaran, K., Rajesh, K. B. and Pillai, T. V. S., Generation of multiple sub wavelength focal spot segments using radially polarized Bessel Gaussian beam with complex phase filter, *Optik-International Journal for Light and Electron Optics*, 125(13), 3159-3161(2014). https://dx.doi.org/10.1016/j.ijleo.2013.12.009

Prentice, P., Cuschieri, A., Dholakia, K., Prausnitz, M. and Campbell, P., Membrane disruption by optically controlled microbubble cavitation, *Nature Phy S.,* 1, 107-110(2005). https://dx.doi.org/10.1038/nphys148

Richards, B. and Wolf, E., Electromagnetic diffraction in optical systems. II. Structure of the image field in an aplanatic system, *Proc. R. Soc. Lond. Ser. A, Math. Phys. Sci.,* 253, 358–379(1959). https://dx.doi.org/10.1098/rspa.1959.0200

Sasaki, K., Koshioka, M., Misawa, H., Kitamura, N. and Masuhara, H., Optical trapping of a metal particle and a water droplet by a scanning laser beam, *Appl. Phys. Lett*., 60, 807(1992). https://dx.doi.org/10.1063/1.107427

Shvedov, V. G., Izdebskaya, Y. V., Rode, A. V., Desyatnikov, A., Krolikowski, W. and Kivshar, Y. S., Generation of optical bottle beams by incoherent white-light vortices, *Opt. Express*, 16(25), 20902–20907(2008). https://dx.doi.org/10.1364/OE.16.020902

Suyama, T. and Zhang, Y., 3D super-resolution fluorescence microscopy using cylindrical vector beams, *Prog. Electromagn. Res. Lett*., 43, 73–81(2013). https://dx.doi.org/10.2528/PIERL13080205

Svoboda, K., Schmidt, C. F. and Schnapp, B. J. and Steven,M., Direct observation of kinesin stepping by optical trapping interferometry, *Nature (London)*, 365,721-727(1993). https://dx.doi.org/10.1038/365721a0

Tachibana, K., Uchida, T., Ogawa, K., Yamashita, N. and Tamura, K., Induction of cell-membrance porosity by ultrasound, *Lancet*, 353(9162), 1409-1415(1999). https://dx.doi.org/10.1016/S0140-6736(99)01244-1

Tadir, Y., Wright, W. H., Vafa, O., Ord, T., Asch, R. H. and Berns, M. W., Micromanipulation of spern by a kaser generated optical trap, *Fertil Steril.,* 52(5), 870-873(1989).

Tovar, A. A., Propagation of Laguerre–Bessel–Gaussian beams, *J. Opt. Soc. Am. A.,* 17(11), 2010–2018(2000). https://dx.doi.org/10.1364/JOSAA.17.002010

Wang, H., Shi, L., Lukyanchuk, B., Sheppard, C. and Chong, C. T., Creation of a needle of longitudinally polarized light in vacuum using binary optics, *Nat. Photonics*, 2, 501–505 (2008). https://dx.doi.org/10.1038/nphoton.2008.127

Wright, W. H., Sonek, G. J., Tadir, Y. and Berns, M. W., *IEEE J. Quantum Electron*., 26(12), 2148-2157(1990). https://dx.doi.org/10.1109/3.64351

Ye, J. Y., Chang, G., Norris, T. B., Tse, C., Zohdy, M. J., Hollman, K. W., O'Donnell, M. and Baker, J. R., Trapping cavitation bubbles with a self-focused laser beam, *Opt. Lett*., 2(18), 2316-2138(2004). https://dx.doi.org/10.1364/ol.29.002136

Youngworth, K. S. and Brown, T. G., Focusing of high numerical aperture cylindricalvector beams, Opt. Express, 7(2), 77–87(2000). https://dx.doi.org/10.1364/OE.7.000077

Zhang, P., Zhang, Z., Prakash, J., Huang, S., Hernandez, D., Salazar, M., Christodoulides, D. N. and Chen, Z., Trapping and transporting aerosols with a single optical bottle beam generated by moiré techniques, *Opt. Lett*., 36(8), 1491–1493(2011). https://dx.doi.org/10.1364/OL.36.001491